Lattice Boltzmann Simulations Comparing Conventional and a Heat Conduction Based Flow-Through PCR Micro-Devices

T. Mautner
SSC San Diego, San Diego, CA, USA, tom.mautner@navy.mil

ABSTRACT

This paper describes the lattice Boltzmann, numerical simulations used to evaluate a conduction-based, polymerase chain reaction (PCR) device for uniformity of the micro channel temperature profile and its velocity field distribution. For comparison purposes, numerical simulations were also performed using conventional PCR configurations. The simulation results demonstrate that in two-dimensions adequate performance of both the conventional and the heat conduction-based PCR systems. However, three-dimensional results indicate that nearly uniform wall temperatures (top, bottom and sides) are required to obtain uniform temperature fields in the PCR micro channels.

Keywords: lattice Boltzmann, PCR, microfluidics, simulations

1 INTRODUCTION

The current design considered for a bioagent detector includes a new heat conduction-based PCR [2] device requiring only two heaters. The two heaters will provide the temperatures required by denaturation and replication while heat conduction in the device substrate will provide the hybridization temperature. Prior to testing the new, heat conduction-based PCR device, numerical simulations were performed to evaluate the device and compare its performance to that of conventional, miniaturized flow-through PCR devices.

The fluid flow and temperature distributions in the PCR devices has been modeled using the lattice Boltzmann method. The lattice Boltzmann (LB) method [4] has been used as a computational fluid dynamics (CFD) tool for well over a decade. Unlike the lattice gas automata (LGA) and molecular dynamics approaches, the LB method simulates a flow system by tracking the evolution of particle distributions, not single particles. It differs from traditional CFD in that LB does not directly solve for the macroscopic variables found in the Navier-Stokes equations. The LB method, due to its kinetic nature, has a linear convection operator, and the local nature of the variables make it well suited for parallel computers. Additionally, the LB method is efficient, stable and allows "easy" implementation of boundary conditions and complicated geometries.

2 NUMERICAL METHOD

The technique used in computing incompressible flows with the LB method involves the time evolution of a density distribution function. The evolution of the Boltzmann equation has seen the development and adoption of the single relaxation Bhatnager, Gross and Krook (BGK) model for the collision operator which simplifies the operator and removes the Galilean invariance and dependence of pressure on velocity. It can be demonstrated that the Boltzmann equation recovers the Navier-Stokes equations via the Chapman-Enskog expansion. The LB method requires two steps, relaxation and streaming. During the relaxation step, distributions at the grid nodes relax to the equilibrium state according to the BGK rule. Then, in the streaming phase, the distribution advects freely at the characteristic velocity to the next node. It should be noted that the order of relaxation and streaming is not important. Once the distribution function is known, the macroscopic velocity and pressure can be calculated from its first two moments.

Building on previous work [3], the lattice Boltzmann BKG model in lattice units has the form

$$f_{\alpha,m}(x+e_\alpha\Delta t, t+\Delta t) - f_{\alpha,m}(x,t) = (1/\tau_m)\left[(f_{\alpha,m}(x,t) - f^{eq}_{\alpha,m}(x,t)\right] + F_T(x,t) \quad m=1,2 \tag{1}$$

where f is the particle distribution and m=1,2 indicate equations for the density and temperature fields.

The relaxation coefficients are given by τ_m and the coupling between the velocity and temperature fields is achieved via the force coupling term F_T.

The numerical simulations used a 9 bit (D9Q2) for two-dimensions and a 19 bit (Q19D3) lattice BGK model in three-dimensions. In this formulation the density, ρ, momentum, ρu, temperature, T, pressure, p, and sound speed, c_s, are determined using the expressions

$$\rho(x,t) = \sum_{\alpha=0}^{18} f_\alpha \qquad \rho u(x,t) = \sum_{\alpha=0}^{18} f_{\alpha,1} e_\alpha \tag{2}$$

$$T(x,t) = \sum_{\alpha=0}^{18} f_{\alpha,2} \quad p = c_s^2 \rho \qquad c_s = c/\sqrt{3} \quad c = 1$$

The quantity c=1 indicates that in lattice Boltzmann units, the time and grid spacing are related by $\Delta x = c\Delta t$.

In the current formulation, the temperature, T, evolves according to

$$f_{\alpha_m,2}^{eq} = \frac{1}{6}\left[1 + 2\frac{(e_\alpha \cdot u)}{c}\right] T(x,t) \quad \alpha_m = 1,....,6 \tag{3}$$

Additionally, the viscosity and relaxation parameters for flow field, τ_v, and temperature, τ_T, have expressions which depend on the reference velocity and length, Reynolds number, viscosity and diffusion coefficient, D_T.

$$\nu = \frac{U_{in} L}{\mathrm{Re}} \qquad \tau_\nu = \frac{6\nu + 1}{2} \qquad \tau_T = \frac{6D_T + 1}{2} \tag{4}$$

3 BOUNDARY CONDITIONS

The boundary conditions used in the simulations specify the Reynolds number, fluid viscosity and diffusion coefficient. Equating the Reynolds number at full scale with the Reynolds number in lattice units provides the reference velocity, U_{in}, and the viscosity, ν, which can then be computed using the equations given above.

A pressure driven flow can be achieved by specification of the inlet and outlet densities where $\Delta p = c_s^2 \Delta\rho$. Alternatively, the flow may also be driven by application of a forcing term applied at each node whose magnitude is based on the pressure gradient in Poiseuille flow.

Additionally, the inlet and outlet velocities are specified. The inlet velocity components are (U_{in},0,0), and at the outlet the velocity is specified to have a zero gradient flow. The no-slip velocity boundary condition is applied to the channel walls using the bounce back technique in the LB formulation.

Finally, the wall temperature distribution is also specified on the boundary nodes, and the boundary temperature is obtained using the extrapolation procedure given by the equation

$$f_{\alpha,2}(\bar{x}_b, t) = f_{\alpha,2}^{eq}(\bar{x}_b, t) + f_{\alpha,2}(\overline{\overline{x}}_{b+1}, t) - f_{\alpha,2}^{eq}(\overline{\overline{x}}_{b+1}, t) \tag{5}$$

4 TEMPERATURE-FLUID COUPLING

The forcing function, F_T, which provides the thermal-velocity coupling, can be computed using several parameters, the Rayleigh number, Ra, the viscosity, ν, the Prandtl number, Pr and the reference length, L.

The magnitude of the forcing term will be determined using specific sets of variables depending upon if it is free or forced convection flow. Examination of the Nusselt number, Nu, indicates that for forced convection Nu=Nu(Re,Pr) and for free convection Nu=Nu(Re,Pr,Gr) where Re is the Reynolds number and Gr is the Grashof number. Typical values of constant portion of the forcing term range from $5.6\text{x}10^{-6} \le F_T \le 5.6\text{x}10^{-4}$ for z=25 grid cells and $5.6\text{x}10^{-5} \le F_T \le 5.6\text{x}10^{-3}$ for z=10 grid cells.

5 RESULTS

The lattice Boltzmann numerical scheme described above was used to compute the velocity and temperature fields in two- and three-dimensional geometries. The microchannel geometry used is a representative section of a serpentine, continuous, flow-through PCR device having various aspect ratios and various corner configurations.

It was apparent early in the investigation that there were significant differences in the two- and three-dimensional simulation results. Straight and U-channels results demonstrate the effects of specified wall temperature distributions for both conventional and the conduction based flow-through PCR systems. The results, in the examples below, are given at time steps of 10K-20K.

5.1 Conventional PCR – Straight Channels

The first set of simulation results are presented in Figure 1 and illustrates the typical results obtained for three-dimensional simulations of conventional flow-through PCR. Conventional PCR in this context adheres to the notion of constant fluid heating in each temperature zone. The use of small thermal-fluid coupling, Figure 1a, results in nearly uniform temperature fields. However, specification of a larger thermal coupling force provides natural convection like effects resulting in significant non-uniform temperature fields as shown in Figure 1b. It should be noted that in these two cases, the bottom and side walls have the same temperature while the top wall has 0.95T of the bottom wall.

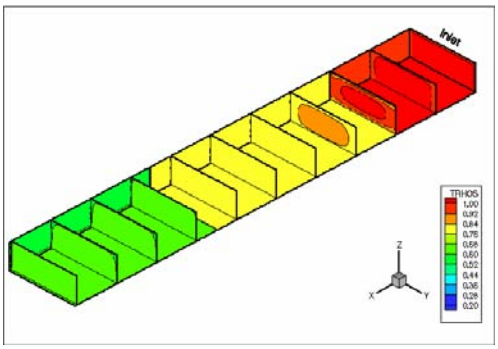

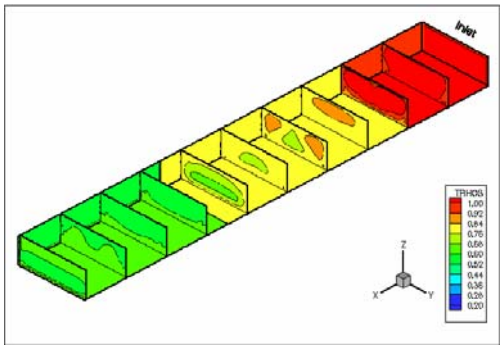

Figure 1. Straight channel section with aspect ratio of 3:1, Re=0.10 and grid (x,y,z)=200x32x10. From inlet to outlet, the specified wall temperatures are: bottom, T=1.0, 0.83, 0.63; top and sides, T=0.95T of bottom. (a) F_T=0.000056; (b) F_T=0.0056

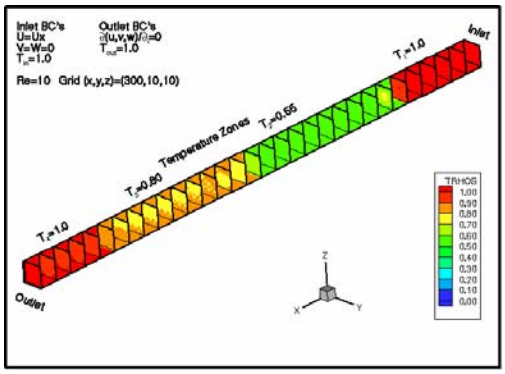

Figure 2. Straight long channel section with aspect ratio of 1:1, Re=10, grid (x,y,z)=300x10x10, and F_T=0.000056. From inlet to outlet, the specified wall temperatures are: bottom and sides, T=1.0, 0.55, 0.80, T=1.0; top, T=0.95T of bottom.

The example, shown in Figure 2, illustrates the application of nearly uniform wall heating on a very long, square channel. The resulting fluid temperature is reasonably uniform except in the T=0.80 zone. This non-uniformity may be the result of having to abruptly transition from T=0.55 to T=0.80 in a short length of channel. Comparison of the results for Re=0.1-10 shows very little difference in the temperature contours over this range of Reynolds numbers.

As observed for straight channels, applying the same temperature on all walls of a U channel aids in providing a nearly uniform fluid temperature as demonstrated in Figure 3a. However, the problem of transitioning from the mid temperature T=0.575 to T=0.825 remains. The results also show the rotational flow due to the relatively small temperature gradient field in the T=0.825 region. The rotational flow does not help to completely mix the fluid temperature.

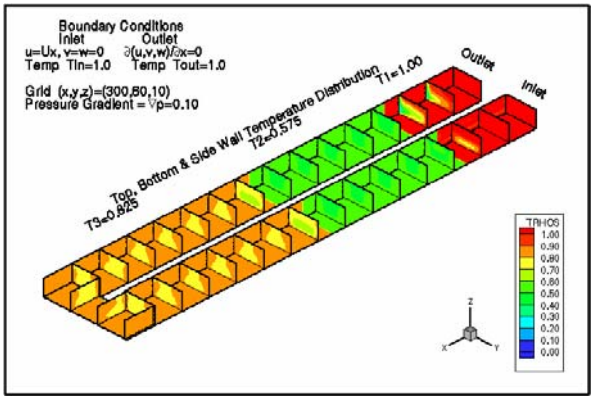

Figure 3. Temperature contours for a long U channel section with aspect ratio of 2:1, Re=0.1, grid (x,y,z)=300x60x10, and F_T=0.0056. From inlet to outlet, the specified wall temperatures are: bottom, top and sides, T=1.0, 0.575, 0.825, 0.575 and 1.0.

5.2 Heat Conduction Based PCR

The next two examples illustrate the effect of two- and three-dimensional geometries on the temperature field for the heat conduction-based PCR system considered for the biosensor design. First, the two-dimensional results are given in Figure 4, and indicate sharp transitions between the various temperature zones. Also, the computed velocity profiles have the expected shape characteristic of Poiseuille flow. These results are in agreement with other simulations found in the literature [1].

In contrast, the three-dimensional simulations using the same wall temperature distributions, shows the effects of volume (geometry) on the resulting flow characteristics, see Figure 5. The problems associated with non-uniform temperature distributions are more significant than those for the conventional PCR configurations. The concern here is that the temperature field will not be sufficient to maintain the sample temperature during each PCR stage during high volume processing. Also, the non-uniform temperature distributions may require longer channels (longer resident times) to achieve proper amplification of the sample.

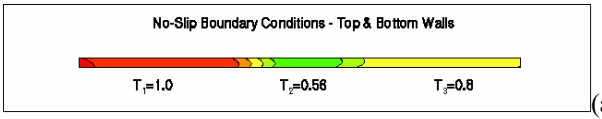

(a)

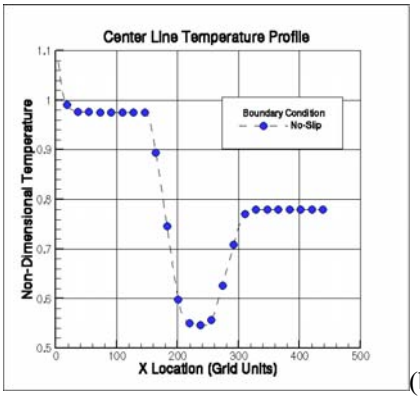

(b)

Figure 4. 2D simulation of the 2-heater PCR device, Re=0.10, time=20K, Grid 450x10, Forcing=0.00056: (a) temperature contours along the channel; (b) the computed centerline temperature distribution (similar to applied wall temperature boundary conditions)

6 SUMMARY

The two-dimensional flow channel results indicated that with nearly equal top and bottom wall temperatures, the PCR device would have essentially uniform temperature profiles across the channel. Thus, one would conclude that the PCR configuration would provide adequate sample amplification. However, the three-dimensional simulations present different findings. The three-dimensional simulations demonstrated that when the top and side wall temperatures were near ambient temperature there would be large temperature gradients and unsatisfactory temperature profiles across the channel. In an attempt to obtain uniform temperature profiles across the three-dimensional channel, various wall temperature distributions were tested. The most favorable temperature profiles consisted of specifying the top and side wall temperature to be on the order of 95-100% of the bottom temperature distribution.

ACKNOWLEDGMENTS

The author thanks the Joint Science & Technology Office for Chemical and Biological Detection for their support. Also, many thanks go to Dr. Peter Gascoyne, MD Anderson Cancer Center, U. Texas Houston and Dr. Shaochen Chen, U. Texas Austin for their continued discussions, encouragement and PCR device data.

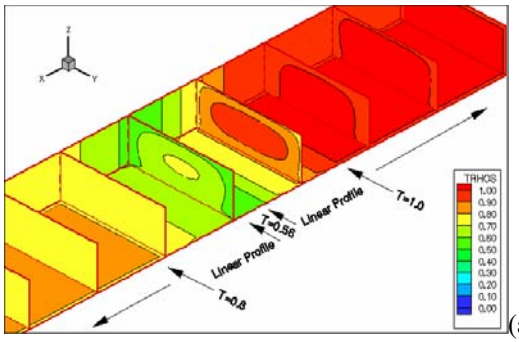

(a)

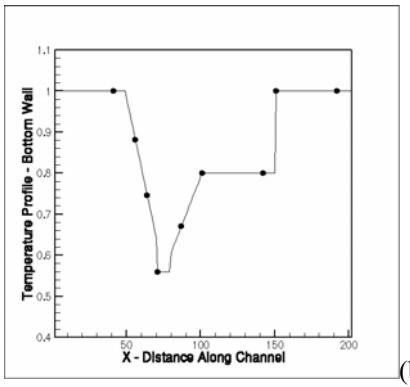

(b)

Figure 5. 3D simulations of the 2-heater PCR device, Re=0.10, time=10K, Grid 200x30x10, Forcing=0.000056: (a) temperature contours in a channel with 4 temperature zones, T=1.0, T=0.56, T=0.8 and T=1.0, close up view of the channel center region temperature distribution; and (b) wall temperature boundary condition.

REFERENCES

[1] Athavale, M., Chen, Z., Furmanczyk, M. and Przekwas, A., "Coupled multiphysics and chemistry simulations of PCR microreactors with active control," Modeling & Simulation Microsystems, 2001.

[2] Li, S. and Chen, S., "Design and analysis of a heat conduction-based continuous flow polymerase chain reaction system," ASME IMECE2002-33548, New Orleans, LA, 2002.

[3] Mautner, T. , "Investigation of enhanced mixing in microfluidic flows using lattice Boltzmann simulations of velocity and temperature fields," World Congress on Medical Physics and Biomedical Engineering, Sydney, AU, Aug., 2003.

[4] Succi, S., 2001, *The Lattice Boltzmann Equation for Fluid Dynamics and Beyond*, Clarendon Press, Oxford.